2011 International Symposium on Nonlinear Theory and its Applications
NOLTA2011, Kobe, Japan, September 4-7, 2011

Efficiency Analysis of Signal Response in Coupled Inferior Olive Neurons with Velarde-Llinás model

Sou Nobukawa†, Haruhiko Nishimura † and Naofumi Katada †

†Graduate School of Applied Informatics, University of Hyogo
7-1-28, Minatojima-minami, Chuo-ku, Kobe, Hyogo, 650-0047 Japan
Email: ab10y406@ai.u-hyogo.ac.jp, haru@ai.u-hyogo.ac.jp, nkatada@hyogo-c.ed.jp

Abstract—Schweighofer *et al*. have demonstrated in computer simulation for their Hodgkin-Huxley(HH) type compartmental model that chaotic irregular firing can be produced in the inferior olive(IO) network, and rich error signals for efficient cerebellar learning may be allowed by this chaotic effect. In this paper, we focus on the Velarde-Llinás IO neuron model which is consistent with experimental data in all main features of IO neuron membrane potential dynamics and is much simpler than HH model. We investigate the signal response of IO assembly in both cases of chaotic resonance and stochastic resonance under the condition for sustaining IO neuron properties.

1. Introduction

The cerebellum is the system of motor control and its function is acquired by cerebellar learning for adapting the change of outside environments. In the cerebellar learning process, the inferior olive (IO) cells transmit error signals to the Purkinje cells through the climbing fibers. The synaptic weights between the parallel fibers and the Purkinje cells are adjusted by long term depression (LTD) due to input of the error signals [1, 2, 3]. Each error signal must carry a sufficient amount of information for the cerebellar learning for efficient motor control, but then the firing rate of IO neuron is known to be very low (< 1 [Hz]). It has been recognised that this low firing rate apparently contradicts the error signal with high temporal resolution.

Schweighofer *et al*. constructed a IO neuron model which is Hodgkin-Huxley (HH) type compartment system composed of a soma and a dendrite[4]. Their simulation study showed that chaotic irregular firings produced in the network of this IO neuron model can transmit rich error signal with low firing rate[5]. This phenomenon is not the conventional stochastic resonance (SR)[6] by noise, but chaotic resonance (CR)[7, 8] enhancing signal responses by chaos. There is also experimental evidence to support this firing [9, 10].

By the way, Llinás *et al*. [11] has proposed a simpler model than HH type one, which is focused on the membrane potential behavior and the dynamics (We call this model Velarde-Llinás model from now on). The characteristics of signal responses in CR and SR of this model have not been studied. In this paper, we examine the response to a periodic signal in the coupled Velarde-Llinás IO neuron assembly and clarify its efficiency in CR and SR under the conditions of IO neuron's low firing rate and the asynchronous firing among IO neurons.

2. Model and Methods

2.1. Velarde-Llinás Inferior Olive Neuron Model and Its Interaction

Velarde-Llinás IO neuron model is a system composed of Van der Pol (VP) sub-system, high threshold FitzHugh-Nagumo(FNI) sub-system and low threshold FitzHugh-Nagumo(FNII) sub-system to reproduce the membrane potential behavior which is observed experimentally such as sub-threshold oscillations and spike generation at two different thresholds[12]. Figure 1 shows that each sub-system is coupled by parameters α, β and h, when the coupling strength between VP and FNI is set to 1 (normalized). This model is described as follows:

$$x' = y, \quad y' = (\gamma(1+\alpha u) - x^2)y - \omega^2(1+\beta u)x, \tag{1}$$

$$\varepsilon w' = g(w) - z - x, \quad z' = 0.5(w - I_2)(w^2 + 0.1), \tag{2}$$

$$\varepsilon u' = f(u) - v + hw,$$

$$v' = 0.05(u - I_1)(u^2 + 0.5), \tag{3}$$

where $(x, y), (w, z), (u, v)$ are variables of VP , FNI and FNII respectively. Here, the functions of f and g which determine the characteristic of threshold in FN sub-systems are given by

$$f(u) = \begin{cases} -1.5u & (u < a) \\ 0.2u - 1.7a & (a < u < 4) \\ -1.6u - 1.7a + 7.2 & (u > 4) \end{cases}, \tag{4}$$

$$g(w) = \begin{cases} -2w & (w < b) \\ 3w - 5b & (b < w < 1) \\ -5w - 5b + 8 & (w > 1) \end{cases}, \tag{5}$$

where a and b determine the high threshold and the low threshold respectively.

In our simulations we adopt two types of assembly similar to ones used by Schweighofer *et al*.[5] as shown in Fig. 2. The type of (a) is the chain assembly of 10 neurons in

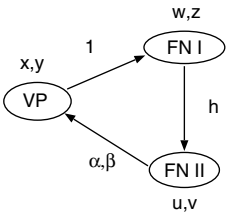

Figure 1: Constitution of Velarde-Llinás IO neuron model. VP: Van der Pol sub-system, FN I: Low threshold FitzHugh-Nagumo sub-system, FN II: High threshold FitzHugh-Nagumo sub-system.

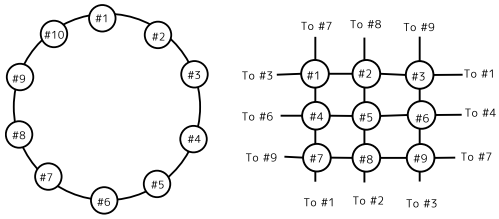

(a) Chain type (b) Lattice type

Figure 2: Configuration of IO neuron assembly.

which each neuron couples its two nearest neighbors. The type of (b) is the lattice assembly of 3×3 neurons in which each neuron couples its four nearest neighbors. Here each neuron couples through FNII sub-systems with a gap junction described as the difference among membrane potentials of coupled neurons. In the chain assembly the equation for u' in Eq. (3) is replaced by

$$\varepsilon u_i' = f(u_i) - v_i + hw_i + J(u_{i+1} + u_{i-1} - 2u_i), \tag{6}$$

where u_i represents the membrane potential of the i-th neuron ($i = 1, 2, \cdots 10$) and J is the coupling strength of the gap junctions.

In the lattice assembly the equation for u' becomes

$$\varepsilon u_i' = f(u_i) - v_i + hw_i + J(u_j + u_k + u_l + u_m - 4u_i), \tag{7}$$

where u_i represents the membrane potential of the i-th neuron ($i = 1, 2, \cdots 9$) and u_j, u_k, u_l and u_m are the membrane potentials of four nearest neighbors. Here the periodic boundary condition is applied to these assemblies.

To evaluate the signal response of Velarde-Llinás IO neuron assembly, we consider a weak periodic signal $S(t) = A \sin 2\pi f_0 t$ and a gaussian white noise $D\xi(t)$ ($< \xi(t) >= 0, < \xi(t), \xi(t') >= \delta_{tt'}$) for Eqs. (6) and (7) as follows:

$$\begin{aligned}\varepsilon u_i' &= f(u_i) - v_i + hw_i \\ &\quad + J(u_{i-1} + u_{i+1} - 2u_i) + S(t) + D\xi(t),\end{aligned} \tag{8}$$

$$\begin{aligned}\varepsilon u_i' &= f(u_i) - v_i + hw_i \\ &\quad + J(u_j + u_k + u_l + u_m - 4u_i) + S(t) + D\xi(t).\end{aligned} \tag{9}$$

In the case of CR, noise is absent ($D = 0$), and in the case of SR noise is applied ($D \neq 0$).

2.2. Evaluation Indices

To quantify the signal response, we use the following four indices. The mutual correlation $C(\tau)$ between the cycle histogram $F(\tilde{t})$ of the neuron spikes and the signal $S(\tilde{t})$ is given by

$$C(\tau) = \frac{C_{SF}(\tau)}{\sqrt{C_{SS} C_{FF}}}, \tag{10}$$

$$\begin{aligned}&C_{SF}(\tau) \\ &=< (S(\tilde{t} + \tau) - < S(\tilde{t}) >)(F(\tilde{t}) - < F(\tilde{t}) >) > .\end{aligned} \tag{11}$$

$F(\tilde{t})$ is a histogram of firing counts at $t_k \mod (T_0)$ ($k = 1, 2, \cdots$) against the signal $S(\tilde{t})$ with a period $T_0 (= 1/f_0)$, $0 \leq \tilde{t} \leq T_0$. For the time delay factor τ, we check $\max_\tau C(\tau)$, i.e., the largest $C(\tau)$ between $0 \leq \tau \leq T_0$.

As an index of synchronization of spikes in the assembly, the coherence measure[13] is utilized. The coherence between two neurons i and j is measured by the following equation:

$$K_{ij} = \frac{\sum_{l=1}^{m} X(l) Y(l)}{\sqrt{\sum_{l=1}^{m} X(l) \sum_{l=1}^{m} Y(l)}}. \tag{12}$$

$X(l)$ ($l = 1, 2 \cdots, m$ $(T/m = \Delta t)$) is the spike train of the i-th neuron during a long term interval T and given by 0 or 1. Here, if the i-th neuron fires within the l-th time bin, $X(l) = 1$ otherwise $X(l) = 0$. $Y(l)$ for the j-th neuron is given in the same way. In the simulation, we take $T = 100T_0$ and $\Delta t = 10$. The population coherence of the whole assembly is obtained by the average of K_{ij} over all pairs of neurons:

$$K = \frac{2}{N(N-1)} \sum_{i=1}^{N} \sum_{j<i} K_{ij}, \tag{13}$$

where N is the number of neurons in the assembly.

To evaluate the physiological validity of the firing rate, we introduce the firing frequency to sub-threshold oscillation frequency ratio (FSR). Because the firing frequency of IO neuron is normally around or lower than 1 [Hz] and the sub-threshold oscillation is about 10 [Hz], FSR becomes smaller than 0.1[14]. Even if IO neuron spikes at every sub-threshold oscillation, FSR does not over the limit of 1.0.

We also use the maximum Lyapunov exponent λ_1 to evaluate the chaos in the system.

Simulation parameters $\varepsilon, \gamma, \omega^2, I_1, I_2, \alpha, \beta, a, b$ and f_0 are kept to $\varepsilon = 0.01, \gamma = 0.21, \omega^2 = 0.63, I_1 = 0.9, I_2 = -0.7, \alpha = 0.95, \beta = 0.9, a = 1.8, b = 0.5$ and $f_0 = 10^{-2}$ throughout our simulations.

3. Results and Discussion

3.1. Chaotic Resonance

This section concerns the deterministic response of the system in the case of noise-free ($D = 0$). The parameter h

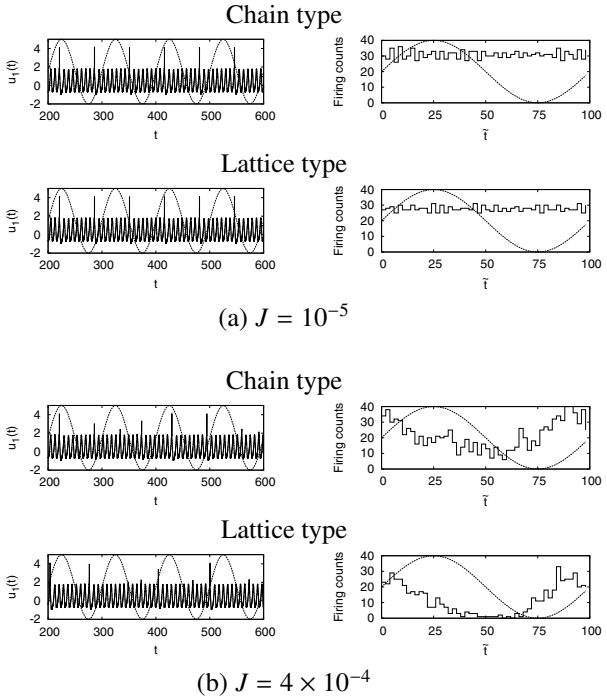

(a) $J = 10^{-5}$

(b) $J = 4 \times 10^{-4}$

Figure 3: Time series of membrane potential $u_1(t)$ (left) and corresponding cycle histogram $F(\tilde{t})$ (right) under the sinusoidal input signal $S(\tilde{t})$ (dotted line). (a) for $J = 10^{-5}$, (b) for $J = 4\times10^{-4}$ in chain and lattice types. ($h = -3.108, \alpha = 0.95, \beta = 0.9, I_1 = 0.9, I_2 = -0.7, f_s = 0.01, A = 10^{-3}$).

is taken as -3.108 where the membrane potential u_i spikes periodically when the IO neurons are uncoupled ($J = 0$). Figure 3 shows the time series of $u_1(t)$ which is the first neuron of the coupled assembly and the corresponding cycle histogram $F(\tilde{t})$ of firing counts under the condition of a weak signal strength ($A = 10^{-3}$). In the case (a) $J = 10^{-5}$, the neurons still fire periodically and the cycle histogram $F(\tilde{t})$ does not respond to the signal $S(\tilde{t})$ in both chain and lattice types. However, by increasing coupling strength J to appropriate one, the neurons become to fire aperiodically and the cycle histogram $F(\tilde{t})$ fits to the signal $S(\tilde{t})$ with some time delay τ as shown in (b) $J = 4 \times 10^{-4}$. Beyond the appropriate region of J, the assembly loses the signal response.

Let us examine the J dependence of the evaluation indices introduced in 2.2 for the above data. Figure 4 indicates J dependence of $\max_\tau C(\tau)$, K, FSR and λ_1. The $\max_\tau C(\tau)$ peaks near 0.9 at around $J = 4\times10^{-4}$. In this region, the firing rate is low ($FSR \approx 0.1$), the neurons in the assembly fire asynchronously ($K \approx 0.2$) and the assembly has a chaotic state ($\lambda_1 > 0$).

From these results, It is found that the appropriate coupling strength J leads the assembly to the asynchronous chaotic firing state and then the response to the signal $S(t)$ is enhanced owing to this activity. This signal response can be interpreted as CR.

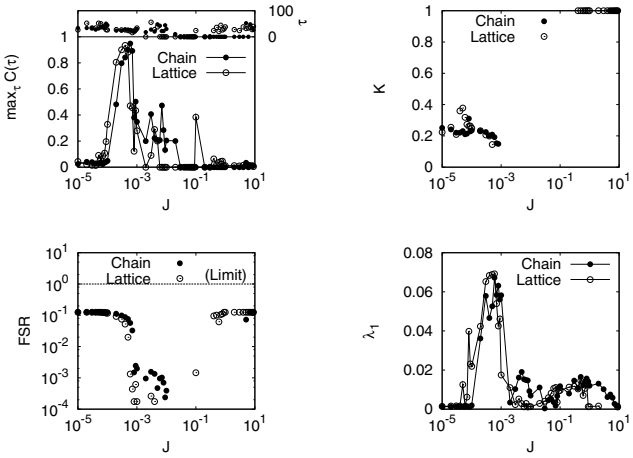

Figure 4: Dependence of evaluation indices on coupling strength J in CR case. ($h = -3.108, \alpha = 0.95, \beta = 0.9, I_1 = 0.9, I_2 = -0.7, f_s = 0.01, A = 10^{-3}$).

3.2. Stochastic Resonance

We also examine the stochastic response of the system with noise ($D \neq 0$). The parameter h is taken as -1.3 where the membrane potential $u_i(t)$ cannot spike and takes sub-threshold periodic oscillation when IO neurons are noise-free ($D = 0$) and uncoupled ($J = 0$). Then the signal strength A of $S(t)$ is set to 0.1 that is a sub-threshold value keeping a non-firing state but much larger than 10^{-3} in CR case. Figure 5 shows the D dependence of $\max_\tau C(\tau)$, K and FSR in the cases of $J = 10^{-5}, 10^{-3}$ and 10^{-1} in the chain and lattice type assemblies. Indeed $\max_\tau C(\tau)$ peaks at $D \approx 0.1$ but the firing rate is too high ($FSR \approx 1.0$) and the neurons fire almost synchronously ($K \approx 0.8$) in both chain and lattice types. This indicates that the conventional SR can occur in the situation inappropriate for the physiological observation in the cerebellar learning. We could manage to tune D to the conditions (when $D \approx 0.06$, $\max_\tau C(\tau) \approx 0.8$, $FSR \approx 0.02$ and $K \approx 0.2$). However, u_1's behavior of the sub-threshold oscillation at $D = 0.06$ is much noisy compared to the physiological observation as shown in Fig. 6 (a). By decreasing D to around 0.02, the sub-threshold oscillation can be sustained as shown in Fig. 6 (b), but then the value of 0.02 is too weak for the assembly to respond to the signal.

4. Conclusion

In this paper, we have examined the efficiency of CR and SR as the signal response in the coupled Velarde-Llinás IO neuron assembly taking into account the conditions of IO neuron's low firing rate and the asynchronous firing among IO neurons which are well known in the cerebellar learning process. From the results, CR is found to have the high efficiency and be consistent with above conditions. On the contrary, SR is confirmed to be obliged to lose the effi-

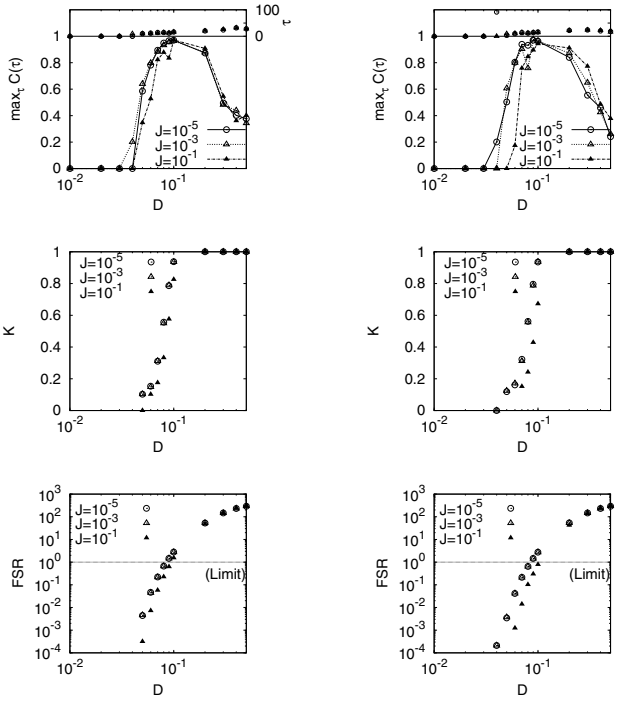

(a) Chain type (b) Lattice type

Figure 5: Dependence of evaluation indices on noise strength D in SR case. ($h = -1.3, \alpha = 0.95, \beta = 0.9, I_1 = 0.9, I_2 = -0.7, A = 0.1, f_s = 10^{-2}$).

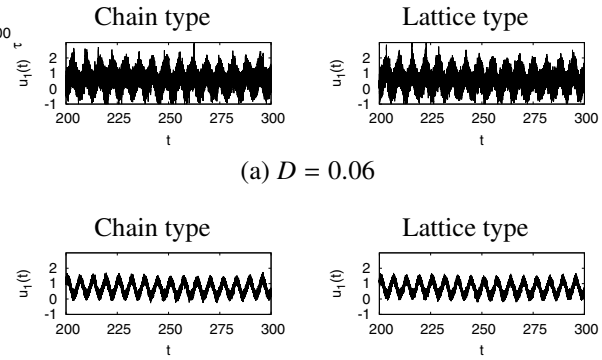

(a) $D = 0.06$

(b) $D = 0.02$

Figure 6: Time series of $u_1(t)$ in SR case. (a) for noise strength $D = 0.06$, (b) for $D = 0.02$. ($J = 10^{-3}, h = -1.3, \alpha = 0.95, \beta = 0.9, I_1 = 0.9, I_2 = -0.7, A = 0.1, f_s = 10^{-2}$).

ciency in the signal response on account of noise restriction. Similar results are also obtained in large scale IO neuron assemblies up to 10^4 neurons. It is concluded that CR can play a role of the signal response mechanism in the real IO neuron assembly but SR cannot. A further direction of this study will be to evaluate the effect a weak background noise allowed for the actual IO on the signal response in CR.

References

[1] D. Marr, "A theory of cerebellar cortex", J. Physiol. (Lond.), vol. 202, pp.437-470 , 1969.

[2] J. S. Albus, "A theory of cerebellar function", Math. Biosci., vol. 10, pp.25-61, 1971.

[3] M. Ito, M. Sakurai and P. Tongroach, "Climbing fiber induced depression of both mossy fibre responsiveness and glutamate sensitivity of cerebellar Purkinje cells", J. Physiol. (Lond.), vol. 324, pp.113-134 , 1982.

[4] N. Schweighofer, K. Doya, M. Kawato, "Electrophysiological Properties of Inferior Olive Neurons: A Compartmental Model", J. Neurophysiol , vol. 82, pp. 804–817, 1999.

[5] N. Schweighofer, K. Doya, H. Fukai, J. V. Chiron, T. Furukawa, M. Kawato, "Chaos may enhance information transmission in the inferior olive", PNAS, vol. 101, no. 13, pp. 4655-4660, 2004.

[6] L. Gammaitoni, P.Hänggi, P. Jung, F. Marchesoni, "Stochastic resonance", Reviews of Modern Physics, vol. 70, no. 1, pp.223–287, 1998.

[7] V. S. Anishchenko, A. B. Neiman, M. A. Safanova, "Stochastic Resonance in Chaotic System", J. Stat. Phys. , vol. 70, pp.183–196, 1993.

[8] H. Nishimura, N. Katada, K. Aihara, "Coherent Response in a Chaotic Neural Network", Neural Processing Letters, vol. 12, no. 1, pp.49–58, 2000.

[9] Y. Kobayashi, K. Kawano, A. Takemura, Y. Inoue, T. Kitama, H. Gomi, M. Kawato, " Temporal Firing Patterns of Purkinje Cells in the Cerebellar Ventral Paraflocculus During Ocular Following Response in Monkeys II. Complex Spikes", J. Neurophysiol., vol. 80, pp.823-848, 1998.

[10] S. Kitazawa, D. M. Wolpert, "Rhythmicity, randomness and synchrony in climbing fiber signals", TREND in Neurosciences, vol. 28, no. 11, pp. 611–619, 2005.

[11] M. G. Velarde, V. I. Nekorkin, V. B. Kazantsev, V. I. Makarenko, R. Llinás, "Modeling inferior olive neuron dynamics", Neural Networks, vol. 15, no. 1, pp.5–10, 2002.

[12] R. Llinás, Y. Yarom, "Oscillatory properties of guinea-pig inferior olivary neurones and their pharmacological modulation", J. Physiology, vol. 376, pp.163–182, 1986.

[13] X-J. Wang, G Buzsáki , "Gamma Oscillation by Synaptic Inhibition in a Hippocampal Interneuronal Network Model", J. Neuroscience, vol. 16, no. 20, pp. 6402–6413, 1996.

[14] A. Latham, D. H. Paul, "Spontaneous activity of cerebellar Purkinje cells and their responses to impulses in climbing fibres" , J. Physiology (London), vol. 212, pp.135–156, 1971.